CHEMISTRY
A EUROPEAN JOURNAL

DOI: 10.1002/chem.200601189

Imaging with Chemical Analysis

Imaging with Chemical Analysis: Adsorbed Structures Formed during Surface Chemical Reactions

Andrea Locatelli and Maya Kiskinova*[a]

Abstract: Imaging surfaces and interfaces with structural and chemical specificity has been essential for understanding a variety of phenomena occurring in adsorbed layers during surface chemical reactions. A recent achievement of chemical imaging with spectroscopic analysis is the experimental proof of theoretically predicted spontaneous formation of regular patterns of metal adatoms during surface chemical reactions. An attractive feature of this finding is that the reaction rate and adlayer coverage can be employed to precisely control the morphology of the structures. The mechanisms of these self-organisation phenomena, driven by the interplay between energetic principles and kinetics, opens a conceptually novel route to creating a wide range of surface-supported functional structures at the micro- and nanometre length scales.

Keywords: adsorption · chemical imaging · non-equilibrium processes · photoelectron spectroscopy · self-assembly · surface chemistry

Introduction

Surface chemical reactions governed by nonlinear kinetics sustain the development of non-equilibrium spatiotemporal travelling or stationary reaction–diffusion patterns.[1,2] These are adsorption structures dynamically created, modified and annihilated by the propagation of chemical reaction fronts. The intrinsic interest in self-organisation processes has driven rigorous studies of pattern formation on metal catalyst surfaces, for which an extremely rich variety of different structures has been reported.[3] These studies revealed that the length scale of adsorbate structures formed only by the interplay between reaction and diffusion is set by the diffusion length of the involved species and typically lies in the μm range.[3–5] Formation of patterns on shorter sub-μm scales has been observed in the presence of strong lateral interactions between the reactants and/or structural reorganisation at the substrate surface.[6–8] Often the interaction between the constituents in these reaction systems favours phase separation processes. As recently demonstrated, chemical "freezing" of the phase separation can sustain spontaneous formation of regular patterns far from thermodynamic equilibrium.[9,10]

Substantial progress in understanding the properties of reaction–diffusion systems has been made by direct imaging using photoemission electron microscopy (PEEM).[11] In this article we review and comment how the fast progress in spatially resolved chemical imaging has contributed to unveiling the mechanisms of "self-organisation" events by following the spatial evolution of complex multicomponent systems in real time. The selected representative systems illustrate the redistribution of adatoms enabled by surface chemical reactions leading to formation of stationary patterns of different local composition, structure and size. A major conceptual advance is that the conditions sustaining spontaneous formation of regular structures can be easily controlled by imposing appropriate reaction parameters. These results suggest that "self-organisation" processes can be employed to steer the formation of surface-supported structures of different wavelength and morphology, which can find use as a versatile method for creating functionalised structured surfaces.

Surface Sensitive Imaging Methods with Chemical Analysis

A limitation of conventional laboratory PEEM is that the photons provided by deuterium or mercury lamps have low energy (<6 eV). Consequently, PEEM can only probe the local work function (WF) and cannot provide unambiguous information about the chemical composition of structures

[a] Dr. A. Locatelli, Dr. M. Kiskinova
Sincrotrone Trieste, Area Science Park
Basovizza, 34012 Trieste (Italy)
Fax: (+39) 040-375-8565
E-mail: kiskinova@elettra.trieste.it

developed during self-organisation processes. This lack of chemical sensitivity can be easily overcome by using very intense and tunable synchrotron sources in the soft X-ray range (e.g., 50–1000 eV) for excitation of the atomic electron core levels. The X-ray PEEM (XPEEM) instruments developed at the third-generation synchrotron facilities today provide the necessary quantitative information about the variations in the chemical composition of interfaces with submicrometer resolution.[12] Implementing energy filtering of emitted electrons adds X-ray photoelectron spectroscopy capability to XPEEM.[12–15] The electron energy analyser allows the obtainment of chemical maps with XPEEM by direct imaging of emitted core level electrons, as well as performing XPS analysis from selected microscopic regions (micro-XPS).

Along with XPEEM, another XPS microscope, called a scanning photoemission microscope (SPEM), has been developed.[12] Its working principle is based on demagnification of the incident photon beam by using appropriate photon-focusing optics, and scanning the sample while collecting the emitted and energy-filtered electrons.

The intensity level in XPEEM or SPEM images corresponds to the emission yield from a specific electronic level of the element under consideration. The contrast level reflects variations in the concentration or chemical state of the element of interest; the so-called core-level energy shifts and changes in the valence spectra are the fingerprints of the actual chemical state and electronic structure.[12,13]

An essential step ahead in the characterisation of realistic multicomponent reaction systems is complementing the chemical with structural information by implementation of a low-energy electron microscopy (LEEM) into the energy-filtered XPEEM instrument.[12,14,16] Owing to the high reflectivity of most materials to very low-energy electrons, LEEM provides structural sensitivity with high lateral and time resolution, and thus is ideally suited to monitor dynamical processes. The insertion of contrast apertures at the diffraction plane allows image filtering in the reciprocal space: LEEM can operate in "bright-field" or "dark-field" mode, depending whether the primary or secondary diffracted beam is selected. Another useful imaging method is mirror electron microscopy (MEM), which probes lateral work function differences using very low energy electrons (<2 eV). Micro-LEED and micro-XPD (X-ray photoelectron diffraction) are also available to characterise the local surface.[16]

Chemical Imaging of Reaction–Diffusion Patterns on a Rh(110) Surface

Travelling concentration waves observed during the H_2+O_2 and $NO+H_2$ reactions on the Rh(110) surface are typical reaction–diffusion patterns with length scales ranging from a few to tens of micrometers. Their shape and velocity are controlled by the reaction parameters, that is, pressure and temperature, which in turn control the mobility of the adspecies, their concentration and the substrate surface structure.[17] PEEM, SPEM and LEEM have provided extensive knowledge about the spatiotemporal organisation of adspecies in these simple reaction–diffusion systems.[18–23] In these reactions, the reactants adsorb dissociatively on the Rh surface and the interaction between adsorbed H, O and N atoms leads to H_2O or H_2O+N_2 products, immediately desorbing in the gas phase. Under appropriate conditions, the adsorbates form stationary or moving two-dimensional concentration patterns, which also induce reversible structural transformations of the substrate.[19–21]

The water formation reaction on Rh(110) is bistable and the propagation of reaction fronts induce transitions between the O-covered ("oxidised") and clean ("reduced") surface. The oxygen adatoms react with hydrogen adatoms at the transition of the reduction front. In contrast to the water formation reaction, the $NO+H_2$ reaction on Rh(110) displays spatiotemporal oscillations, manifested as alternating reduction and oxidation fronts. The reduction fronts remove the adsorbed oxygen, leading to a local built up of a N adlayer, whereas the oxidation fronts favour nitrogen recombination to N_2 and desorption, because the coadsorbed oxygen destabilises the bonding of adsorbed N.[17] In brief, the propagating reduction and oxidation reaction fronts cause a switching between an O- and N-covered surface regions, the width of the transition zone, in which O and NO are coadsorbed, depending on the reaction parameters.[19,21] The complex chemistry of $NO+H_2$ reaction, involving the coexistence of O-$(1\times n)$ and N-$(n\times 1)$ reconstructions of the substrate surface with different diffusion anisotropy,[17] leads to a large variety of chemical wave patterns, such as targets and spirals.[2,18,24]

Figure 1 illustrates the capability of combined MEM, micro-LEED and micro-XPS measurements in the characterisation of spatiotemporal oscillatory patterns during the $NO+H_2$ reaction. The reduction fronts are characterised by lower WF and appear dark in MEM, whereas the oxidation fronts, characterised by higher WF, appear bright. Complementary micro-LEED measurements reveal the following sequence in lateral distribution of the adsorption phases within the O-free and O-covered (O-c) regions: N-(3×1), N-(2×1), $NO+$O-c(2×4) and O-c(2×6). As indicated by the arrows, there is correspondence between WF (MEM) contrast and micro-LEED structures, which change with N and O coverage. Quantification of the lateral distribution of the adspecies was possible only by chemical imaging and was first measured with SPEM.[19] Figure 1 (bottom) shows equivalent micro-XPS data obtained using the XPEEM microscope. The N and O 1s core level emission intensity, plotted as a function of time, show the typical oscillations induced by the consecutive propagation of wave fronts. The N 1s intensity decrease always mirrors the O 1s increase (and vice-versa), consistent with the time evolution of the ordered phases observed with micro-LEED. As the XPS intensities change linearly with N and O coverage, the intensities are normalised against the coverage of saturated O and N adlayers. One monolayer (ML) equals the number of surface Rh atoms on the Rh(110) plane.

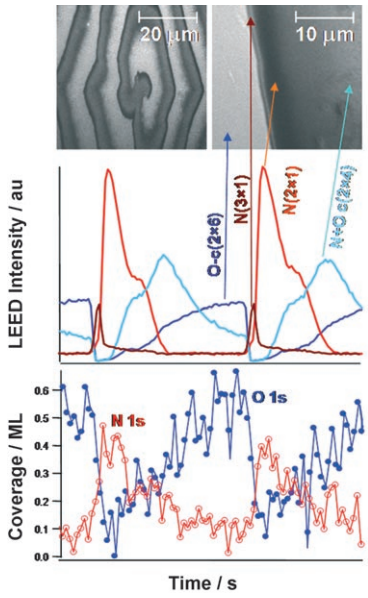

Figure 1. Top: MEM images of the work function variations induced by propagating fronts during the $NO+H_2$ reaction. Centre: Intensity variations of the LEED diffraction spots of developed ordered adsorption structures during wave-front propagation. The arrows indicate the corresponding MEM contrast region. The adsorption structures also involve (3×1), (2×1), (1×2) and (1×3) reconstructions of the Ru(110) substrate, induced by the N, O+N and O adlayers. Bottom: Lateral variations in the N and O 1s core level intensities measured during wave-front propagation, illustrating the dynamics of O and N accumulation/depletion. The maximum intensity of the N 1s and O 1s signal corresponds to the N-(2×1) and O-c(2×6) structures with coverage 0.5 and 0.67 ML, respectively. All measurements were carried out with a combined LEEM-XPEEM instrument.

Chemical Imaging of Redistribution of Modifier Adatoms by Propagating Reaction Fronts

The velocity, shape and wavelength of the reaction–diffusion patterns can be influenced by modifying the structural and chemical properties of the catalyst surface, for example, by adding adatoms of another element we call here "modifier".[25] The "modifier" can steer the catalytic activity and/or selectivity or act as deactivator.[26] Only recently it has been shown that "modifier" adatoms can also participate actively in the pattern formation process.[23,27–34] Such reaction-induced compartmentalisation implies creation of independent chemical microreactors, which can further affect the reactivity and selectivity of the catalyst by maximising or minimising the activation/deactivation effect induced by the modifier. Particularly interesting in this context are systems in which the "modifier" structures, resulting from the reorganisation triggered by the surface reaction, can be stabilised and their wavelengths controlled.[9]

The thoroughly studied simple catalytic reactions, water formation and NO neutralisation on a Rh(110) surface, turned out to be excellent model systems for studying the mechanism sustaining the formation of stationary structures of "modifier" adatoms, which are homogeneously distributed on the surface prior the reaction. Both reactions involve oxygen adatoms as the most strongly bound intermediate species to the Rh surface and their affinity to the modifier adatoms turned out to be an important factor in the observed reorganisation processes.

Stationary Patterns of Alkali Metal Adatoms

The first observations of a mass transport of "modifier" adatoms induced by reaction fronts was reported for the O_2+H_2 and $NO+H_2$ reactions on a Rh(110) surface with submonolayers of K or Cs adatoms.[24,27–29] Alkali metals (AM) are a specific type of "modifier": they are very mobile on metal surfaces and have a very high chemical affinity to so-called electronegative adatoms such as O.[26] In the case of water formation reaction the travelling chemical waves still exist but the front profile and the front velocity are not constant but change continuously. The reason for that is that AMs are transported by the reaction fronts, which leads to the accumulation of AM at the front edge and causes the front velocity to decrease during propagation. Figure 2 illustrates

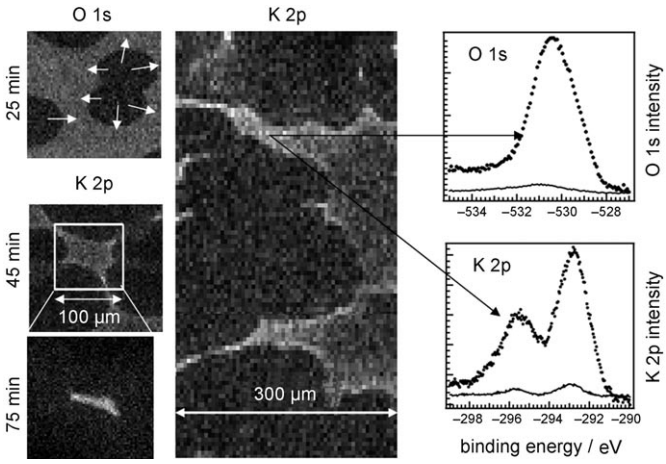

Figure 2. Left: O 1s and K 2p images taken at different reaction times starting from a Rh(110) surface with homogeneous adlayer of 0.75 ML oxygen and 0.08 ML potassium. The arrows indicate the direction of the propagating reduction fronts. Middle: Large area K 2p image of a stationary pattern formed. The bright regions are the K+O islands. Right: O 1s (top) and K 2p (bottom) spectra taken in the K+O islands and in the O-free areas with K residue. The arrows show the spectra corresponding to the dense K+O phase with $\approx$0.25 ML potassium and 0.8 ML oxygen. All measurements were carried out using a SPEM instrument. $P_{O_2}=1.6\times10^{-7}$ mbar, $P_{H_2}=1.6\times10^{-7}$ mbar, $T=570$ K.

how starting from a surface with a homogeneous K+O adlayer, the reduction waves trigger a mass transport of K towards the regions still covered by O. The reaction fronts are thus transients before a stationary K concentration pattern eventually forms.[30] The O 1s and K 2p images and the spectroscopic data confirmed that the K adatoms are compressed into K+O islands, surrounded by areas of an O-free surface with some K residues (see Figure 2).

The characteristic feature of the stationary patterns of condensed K(Cs)+O islands and O-free Rh(110) surface is that they are stable only under water formation reaction conditions, that is, the condensation process is reversible and the patterns are completely dissolved under oxidation or reduction conditions.[27,30] In pure reducing ambient the stationary patterns dissolve much faster than in pure oxidising ambient, because the mobility of K on the clean surface is much higher than on the oxidised one.

The driving force of the reorganisation process ending with formation of stationary patterns is the energy gain of formation of mixed AM+O adsorption phases. The strongly reduced mobility of the AM atoms in the O-covered areas and the reduced reactivity of oxygen coadsorbed with K are key factors in stabilising the morphology and composition of the K(Cs)+O pattern[30,35] In kinetic terms, the presence of "modifier" adatoms determines a "Turing-like" instability of the uniform state and consequent spontaneous generation of spatial concentration patterns. However, the stationary structures observed in these reaction systems are not classic Turing patterns, occurring when the spatially homogeneous state is unstable with respect to a perturbation by diffusion. On AM modified Rh the interactions between AM and O adatoms play a prominent role, that is, the diffusion does not obey the classic Fick's law, but is driven by a gradient in the chemical potential. As shown by kinetic modelling, the "reactive phase separation" process results from non-equilibrium phenomena arising from the interplay between the adsorption process, the diffusion of the adspecies and their mutual lateral interactions.[31,36]

Stationary Patterns of Gold Adatoms

The pattern formation as a result of a phase separation, driven by the high affinity of very mobile alkali metals to oxygen, raised the question whether the reaction-induced reorganisation of species not directly participating in the surface chemical reaction is a general phenomenon. To answer this question we focused our attention on a noble metal modifier, Au.[32–34] During water formation Au is "inert" and also is less mobile relative to K and Cs. The Au adatoms block adsorption sites on the Rh surface, which slows down the water formation reaction rate without affecting the reaction mechanism so that the bistability observed on the Au-free surface is preserved.[25] The transition between the "reduced" and "oxidised" states occurs with propagation of the typical elliptical wave fronts. The LEEM image in Figure 3 shows the development of reduction fronts (bright) followed by concentric re-oxidation fronts (dark) for the specific reaction conditions. XPEEM imaging of the Au 4f core level emission reveals that the ignition and propagation of oxidation fronts trigger reorganisation of the Au adlayer, pushing the Au adatoms towards the O-free areas. At this early reaction stage, the Au re-distribution mimics the elliptical shape of the chemical fronts. This shape is lost in the later stages due to collision of different fronts until a "final" stationary

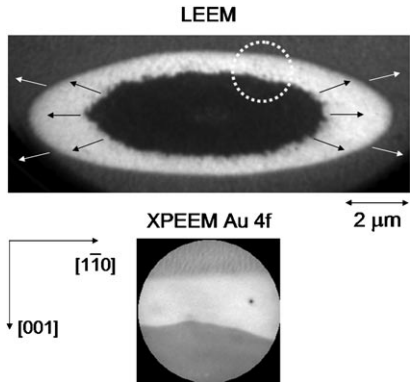

Figure 3. Top: LEEM image of an elliptic reduction front (bright) followed by a concentric oxidation front (dark) after ignition of water formation reaction starting from a homogeneous Au adlayer (0.5 ML) on "oxidised" Rh(110). The front propagation direction is indicated by arrows. Bottom: Au 4f XPEEM image (detail of the wave front), demonstrating Au accumulation into the reduced surface area through mass transport by the oxidation front. $\theta_{Au}=0.6$ ML, $P_{O_2}=2.7\times10^{-7}$ mbar, $P_{H_2}=3.3\times10^{-7}$ mbar, $T=550$ K.

state consisting of alternating Au and O islands is attained. On the basis of combined XPEEM, LEEM and micro-LEED data (Figure 4) it was elucidated that the Au islands contain one ML of Au on a "reduced" unreconstructed Rh-(110) surface, surrounded by O islands of ≈0.5 ML on a missing-row (1×2) reconstructed surface.

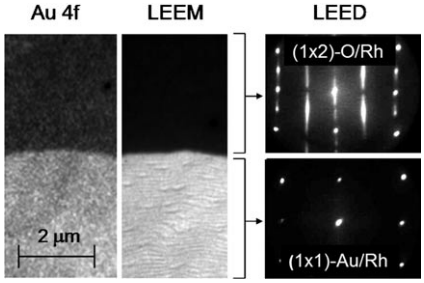

Figure 4. A fragment of a stationary state with alternating Au and O adlayers, created during the water formation reaction on Au-modified Rh (110). From left to right: Au 4f XPEEM image, LEEM image ("bright-field") at 8 eV, and LEED patterns corresponding to Au/Rh and O/Rh structures.

Once the structure–composition relationship is established we employed mostly LEEM to study the time evolution of the interface, as it requires much shorter acquisition times than XPEEM (tens of milliseconds versus seconds). This allowed us to follow the dynamic behaviour of the stationary Au structures under different reaction conditions. In contrast to the case of K(Cs)+O islands described above, the Au islands are preserved under oxidation conditions and dissolved under reduction conditions. An analogous behaviour was observed later for mixed Au+Pd adlayers, in which the reaction triggers phase separation to mixed Au+Pd and O islands.

As in the case of AM modifiers, the observed phase separation in Au/Rh and Au+Pd/Rh systems is driven by energetic principles. Ab initio calculations showed that the mixed Au–O state is energetically less favourable than the

separated Au and O adsorption states, owing to mutual destabilisation of Rh–Au and Rh–O bonds in the coadsorbed phase.[32] Although energetically favoured, the phase separation of gold and oxygen is kinetically hindered in absence of the water formation reaction, because in a static mixed Au+O adlayer the mobility of gold adatoms surrounded by oxygen adatoms is very low. Under reaction, the kinetic hindrance is lifted, because the reaction fronts change dynamically the occupation of surface sites and effectively steer the lateral reorganisation of the adspecies, favoured by the total energy gain.

Formation of Regular Patterns by "Chemically Frozen" Phase Separation

Theoretical studies predict that phase-separating adsorbates can spontaneously reorganise during reaction, leading to formation of regular patterns with well-defined morphology.[5,37,38] The three component kinetic model developed by De Decker and Mikhailov allows analytical study of the growth of spatial modes of modifiers microstructures in the presence of a surface chemical reaction.[9] The wavelength of periodic structures is found to obey power-law dependence on the reaction rate, the instability boundaries of the reaction system being the same as those for spinodal decomposition in absence of a reaction. This implies that the reaction can effectively "freeze" the phase-separation process before macroscopic structures can develop. Thus, the reaction parameters can be used to control the morphology (wavelength and shape) of the adlayer microstructures.

The first experimental demonstration of the "power-law" theoretical predictions for surface chemical reactions was obtained for submonolayer metal adlayers on Rh(110) during water formation reaction. We found that for a relatively narrow temperature range around 800 K and metal adatom coverage 0.45–0.75 ML, regular lamellar structures (Figure 5) spontaneously develop at transition from the "reduced" state, in which metal adsorbates are homogeneously distributed on the surface, to the "oxidised" state, that is, by changing the O_2/H_2 partial pressure ratio. The Au $4f_{7/2}$, Pd $3d_{3/2}$ and O 2p XPEEM images in Figure 6 demonstrate that the lamellae consists of alternating Au+Pd and O islands. In the Rh $3d_{5/2}$ image the contrast is inverted, due to the screening by the Au+Pd adlayer. For comparison of contrast correlations and acquisition times, "bright-field" LEEM and MEM images of the same region are indicated.

The most interesting feature is the observed dependence of wavelength of lamellar patterns, λ, on reaction conditions. In particular the reaction rate that can be finely adjusted by varying the reactants pressure or the reaction temperature can be used as a "tool" for controlling λ. Figure 7 shows a representative example of regular structures formed at different reactant pressures. By increasing the reaction rate at constant temperature and adlayer coverage, we found that the resulting wavelength of the lamellar structures follows a power scaling law, $1/\lambda = kP^n$, over more than two decades

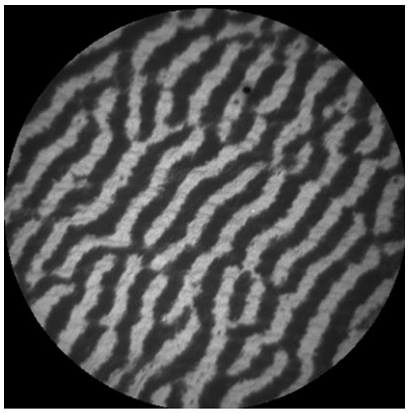

Figure 5. LEEM (8 eV) image of lamellar structures developed on Au+Pd/Rh(110). Reaction parameters: $\theta_{Au+Pd}=0.6$ ML, $P_{O_2}=3.8\times10^{-7}$ mbar, $P_{H_2}=1.9\times10^{-7}$ mbar, $T=780$ K. Field-of-view 20 μm.

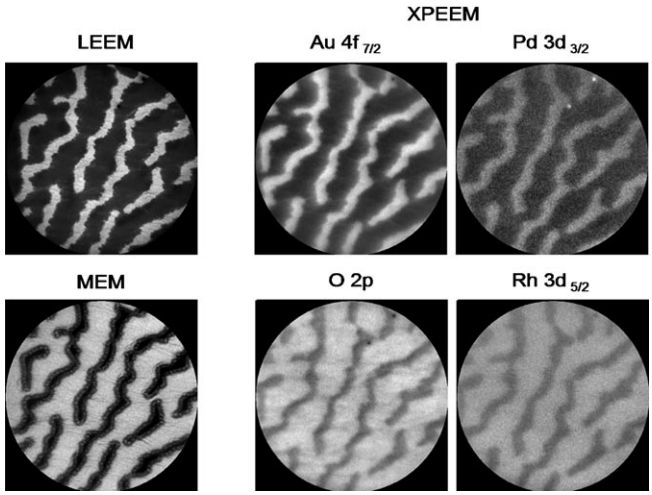

Figure 6. Bright-field LEEM (8 eV). MEM (0.9 eV,) and XPEEM images of lamellar structures developed on a Au+Pd/Rh(110) surface. Regions with high work function, bright in MEM and dark in LEEM, correspond to the "oxidised" (1×2) reconstructed surface. This is confirmed by the XPEEM chemical maps, demonstrating the Au+Pd and O phase separation. Acquisition time:100 ms for LEEM and MEM, 200 s for O 1s and Au 4f maps and 300 s for the Pd 3d and Rh 3d maps. Reaction parameters: $P_{O_2}=3.6\times10^{-7}$ mbar, $P_{H_2}=1.8\times10^{-7}$ mbar, $T=820$ K, $\theta_{Pd+Au}=0.5$ ML, field-of-view 10 μm.

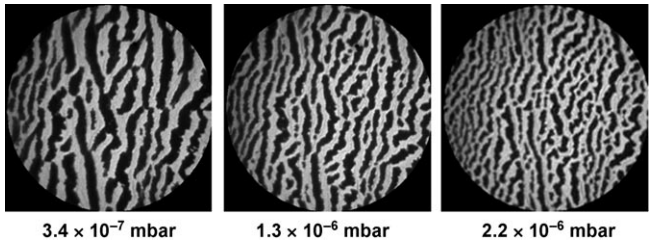

Figure 7. LEEM images (8 eV) of lamellae structures developed at different O_2+H_2 pressures. The wavelength of the structures decreases with increasing reaction rate. Reaction conditions: Au+Pd coverage = 0.75 ML, $P_{H_2}/P_{O_2}=0.8$; $T=820$ K; field-of-view 20 μm.

variation of the reactants pressure. The measured power law exponent, $n = 0.18$ is in fair agreement with theory.[9,10]

The observed "self-organisation", defined as "chemically frozen" spinodal decomposition, and the derived power-law dependence of the structure wavelengths on the reaction rate are common to a broader class of chemically reacting systems. In reacting polymer mixtures spinodal decomposition is suggested as a viable mechanism for structure formation.[39,40] This concept has already been applied to non-equilibrium chemical reactions interconverting two separating polymer species by photoisomerisation, leading to the creation of polymer blends with desired morphologies.[41,42]

The most important feature of the adsorbed microstructures formed by "chemically frozen" phase separation is that they are "adaptive"; that is, they develop and remain stable on the surface only under certain reaction conditions; they can be dissolved and again formed; and their wavelength can be controlled by changing the reaction rate. This would not be possible for any lithographic technique or growth-based fabrication of nanostructures.

Conclusion

The recent development of surface sensitive imaging methods with structural and chemical analysis has opened opportunities to investigate and identify microstructures developed as a result of "self-organisation" processes during surface chemical reactions. Experimentally we were able to create and stabilise periodic metal structures with wavelengths controlled by tuning the reaction parameters; that is, temperature, concentration and pressure. We envisage that these concepts can be further developed and prompt a novel route to formation of surface-supported micro- and nanostructures.

Acknowledgements

We acknowledge the invaluable contribution of Ronald Imbihl and his collaborators and Sebastian Günther who suggested and pioneered the chemical imaging experiments with reaction systems. We thank Alexander Mikhailov, Carlo Sbraccia and Stefano Baroni for their support in interpretation of the results from a theoretical viewpoint and our colleagues Luca Gregoratti, Alexei Barinov, Lucia Aballe, Onur Mentes, Stefan Heun who performed the experiments.

[1] M. Eiswirth, G. Ertl, *Chemical Waves and Patterns*, (Eds.: R. Kapral, K. Showalter), Kluver, Amsterdam, **1995**, p. 447.
[2] R. Imbihl, *Catal. Today* **2005**, *105*, 206–222.
[3] R. Imbihl, G. Ertl, *Chem. Rev.* **1995**, *95*, 697–733.
[4] K. Asakura, J. Lauterbach, H. H. Rotermund, G. Ertl, *J. Chem. Phys.* **1995**, *102*, 8175–8184.
[5] M. Hildebrand, A. S. Mikhailov, G. Ertl, *Phys. Rev. Lett.* **1998**, *81*, 2602–2606.
[6] J. Wintterlin, S. Völkening, T. V. W. Janssens, T. Zambelli, G. Ertl, *Science* **1997**, *278*, 1931–1934.
[7] C. Sachs, M. Hildebrand, S. Völkening, J. Wintterlin, G. Ertl, *Science* **2001**, *293*, 1635–1638.
[8] M. Hildebrand, M. Ipsen, A. S. Mikhailov, G. Ertl, *New J. Phys.* **2003**, 5, 61.1–61.28.
[9] Y. De Decker, A. S. Mikhailov, *J. Phys. Chem. B* **2004**, *108*, 14759–14763.
[10] A. Locatelli, T. O. Mentes, L. Aballe, A. Mikhailov, M. Kiskinova, *J. Phys. Chem. B.*, **2006**, DOI: 10.1021/jp065090u
[11] H. H. Rotermund, W. Engel, M. Kordesch, G. Ertl, *Nature* **1990**, *343*, 355–357.
[12] S. Günther, B. Kaulich, L. Gregoratti, M. Kiskinova, *Prog. Surf. Sci.* **2002**, 70, 187–260, and references therein.
[13] K. Siegbahn, *J. Electron Spectrosc. Relat. Phenom.* **1990**, 51, 11–36.
[14] E. Bauer, *Rep. Prog. Phys.* **1994**, *57*, 895–938.
[15] O. H. Griffith, G. F. Rempfer, *Advances in Optical and Electron Microscopy*, Academic Press, New York, **1987**, p. 26.
[16] T. Schmidt, S. Heun, J. Slezak, J. Diaz, K. C. Prince, G. Lilienkamp, E. Bauer, *Surf. Rev. Lett.* **1998**, *5*, 1287–1296.
[17] M. Kiskinova, *Chem. Rev.* **1996**, *96*, 1431–1447.
[18] F. Mertens, R. Imbihl, *Nature* **1994**, *370*, 124–126.
[19] A. Schaak, S. Günther, F. Esch, E. Schütz, M. Hinz, M. Marsi, M. Kiskinova, R. Imbihl, *Phys. Rev. Lett.* **1999**, *83*, 1882–1885.
[20] F. Mertens, R. Imbihl, *Chem. Phys. Lett.* **1995**, *242*, 221–227.
[21] T. Schmidt, A. Schaak, S. Günther, B. Ressel, E. Bauer, R. Imbihl, *Chem. Phys. Lett.* **2000**, *318*, 549–554.
[22] F. Esch, S. Günther, A. Schütz, A. Schaak, I. G. Kevrekidis, M. Marsi, M. Kiskinova, R. Imbihl, *Surf. Sci.* **1999**, 443, 245–252.
[23] H. Marbach, S. Günther, B. Luerssen, L. Gregoratti, M. Kiskinova, R. Imbihl, *Catal. Lett.* **2002**, 83, 161–164.
[24] F. Mertens, S. Schwegmann, R. Imbihl, *J. Chem. Phys.* **1997**, *106*, 4319–4326.
[25] K. Asakura, J. Luterbach, H. H. Rotermund, G. Ertl, *Surf. Sci.* **1997**, 374, 125–141.
[26] "Poisoning and Promotion in Catalysis Based on Surface Science Concepts and Experiments": M. Kiskinova, in *Studies in Surface Science and Catalysis, Vol. 70* (Eds.: B. Delmon, J. T. Yates), Elsevier, Amsterdam, **1992**.
[27] S. Günther, H. Marbach, R. Hoyer, R. Imbihl, L. Gregoratti, M. Kiskinova, *J. Electron Spectrosc. Relat. Phenom.* **2001**, 114, 989–996.
[28] H. Marbach, G. Lilienkamp, Han Wei, S. Günther, Y. Suchorski, R. Imbihl, *Phys. Chem. Chem. Phys.* **2003**, *5*, 2730–2735.
[29] H. Marbach, S. Gunther, T. Neubrand, R. Imbihl, *Chem. Phys. Lett.* **2004**, *395*, 64–69.
[30] H. Marbach, S. Günther, T. Neubrand, R. Hoyer, L. Gregoratti, M. Kiskinova, R. Imbihl, *J. Phys. Chem. B* **2004**, *108*, 15182–15191.
[31] Y. De Decker, H. Marbach, M. Hinz, S. Günther; M. Kiskinova, A. S. Mikhailov, R. Imbihl, *Phys. Rev. Lett.* **2004**, *92*, 198305–198305.
[32] A. Locatelli, C. Sbraccia, S. Heun, S. Baroni, M. Kiskinova, *J. Am. Chem. Soc.* **2005**, *127*, 2351–2357.
[33] A. Locatelli, A. Barinov, L. Gregoratti, L. Aballe, S. Heun, M. Kiskinova, *J. Electron. Spectrosc. Relat. Phenom.* **2005**, *144*, 361–366.
[34] A. Locatelli, S. Heun, M. Kiskinova, *Surf. Sci.* **2004**, 566–568, 1130–1133.
[35] S. Günther, H. Marbach, R. Imbihl, A. Baraldi, S. Lizzit, M. Kiskinova, *J. Chem. Phys.* **2003**, 119, 12503–12509.
[36] M. Hinz, S. Günther, H. Marbach, R. Imbihl, *J. Phys. Chem. B* **2004**, *108*, 14620–14626.
[37] J. Verdasca, P. Borckmans, G. Dewel, *Phys. Rev. E* **1995**, 52, R4616–R4619.
[38] M. Hildebrand, A. S. Mikhailov, G. Ertl, *Phys. Rev. E* **1998**, 58, 5483–5493.
[39] S. C. Glotzer, E. A. Di Marzio, M. Muthukumar, *Phys. Rev. Lett.* **1995**, *74*, 2034–2037.
[40] M. Motoyama, T. Ohta, *J. Phys. Soc. Jpn.* **1997**, 66, 2715–2715.
[41] Q. Tran-Cong, A. Harada, *Phys. Rev. Lett.* **1996**, *76*, 1162–1162.
[42] Q. Tran-Cong-Miyata, S. Nishigamimi, T. Ito, S. Komatsu, T. Norisuye, *Nat. Mater.* **2004**, *3*, 448–451.

Published online: November 6, 2006

